Distributed Control of Triangular Sensor Formations with Angle-Only Constraints

Meysam Basiri, Adrian N. Bishop and Patric Jensfelt

Royal Institute of Technology (KTH)
Stockholm, Sweden

***Abstract*—This paper considers the coupled formation control of three mobile agents moving in the plane. Each agent has only local inter-agent bearing knowledge and is required to maintain a specified angular separation relative to its neighbors. The problem considered in this paper differs from similar problems in the literature since no inter-agent distance measurements are employed and the desired formation is specified entirely by the internal triangle angles. Each agent's control law is distributed and based only on its locally measured bearings. A convergence result is established which guarantees global convergence of the formation to the desired formation shape.**

***Index Terms*—Angle constraints; bearing-only measurements; distributed control; formation control; multi-agent systems.**

I. Introduction

This paper presents a distributed control system for triangular formation control based only on local bearing measurements and relative angular constraints. The formations considered are characterized entirely by the interior angles subtended at each agent by two neighbor agents. The scenario introduced in this paper is a novel contribution in the field of multi-agent dynamical systems and the control law proposed is provably globally stabilizing.

Distributed control of multi-agent formations has been explored extensively in different settings. For example, consensus and flocking algorithms lead to formation-like steady-state structures of multi-agent systems [1]–[7]. Similarly, so-called aggregation and swarm control, which typically involves potential functions [8], is also common in the robotics and control literature [9], [10]. The problem considered in this paper follows the ideas put forth in [11]–[14]. Specifically we are concerned with the formation, and subsequent maintenance, of specific inter-agent geometric relationships using distributed algorithms. The majority of existing algorithms consider only inter-agent distance measures and constraints. We differ from this in a novel way, by considering only inter-agent bearing measures taken in local coordinates, i.e. agents do not share a common heading. We are motivated by the problem of optimal sensor arrangement for localization [1], [2].

The control laws for formation control can either be distributed or centralized. Often, distributed control lends itself naturally to the multi-agent formation control problem. A distributed law for formation control is implemented by individual agents in the formation. Each agent attempts to achieve (and maintain) the desired relevant constraints placed on it's own position but does not consider the constraints of any other agents (when planning it's own motion control).

This work was supported by the Swedish Foundation for Strategic Research (SSF) through CAS and also via the EU FP7 project 'CogX'.

The contribution of this paper is a distributed law for angular constrained formation control of a multi-agent system where each agent takes only relative bearing measurements. A large literature exists on bearing-only state estimation and localization [15]–[18] which makes the angle-based formation control problem particularly appealing. However, angle-based formation control is not commonly addressed in the literature. Instead, a large literature focuses on distance-based formation control and potential-function-based control laws. In this paper, we introduce an angular constrained formation control problem for a group of agents tasked at maintaining a specified triangular formation. The control law then developed is shown to be globally stabilizing given any initial agent configuration.

The paper is organized as follows. In Section II, the triangular formation control problem is introduced along with the distributed control law proposed in this paper. Subsequently, the multi-agent system evolution is examined and global stability of the desired formation shape is proved. In Section III a number of illustrative examples are given and a conclusion is given in Section IV.

II. Bearing-Only Triangular Formation Control

Consider a group of $n = 3$ agents in $\mathbb{R}^2$ which *interact* via an undirected topology $\mathcal{G} = \{\mathcal{V}, \mathcal{E}\}$ with $\mathcal{V} = \{1, 2, 3\}$ and $\mathcal{E} = \mathcal{V} \times \mathcal{V}$. The position of each agent is $\mathbf{p}_i = [x_i \ y_i]^{\mathrm{T}} \in \mathbb{R}^2$ where x_i and y_i denote agent i's position in the x and y directions respectively. The neighbor set $\mathcal{N}_i \subset \mathcal{V}$ denotes the set of agents connected to agent i by a single (undirected) edge. In this case $\mathcal{N}_i = \{(i+1), (i-1)\}$ (taken modulo n).

Importantly, note that agents do *not* share a common heading, i.e. they are not equipped with a compass of any kind. Agent i measures only the bearing $\phi_{ij} \in [-\pi, \pi)$, $\forall j \in \mathcal{N}_i$ positive (negative) counter-clockwise (clockwise) from their local x_i-direction to agent j. Let α_i denote the angle subtended at agent i by the two agents in $\mathcal{N}_i$. Then, the formation shape (not scale) is completely characterized by α_i, $\forall i \in \mathcal{V}$. Mathematically, the interior α_i is given by

$$\alpha_i \equiv (\phi_{i(i+1)} - \phi_{i(i-1)}) (\mathrm{mod}\ \pi) \tag{1}$$

where $\alpha_i \in [0, \pi]$. Note the difference between $\alpha_i = 0$ and $\alpha_i = \pi$ implies agent i can ascertain whether or not it is in between agents $i+1$ and $i-1$ with all three collinear.

Tacitly, it can be assumed that α_i is measured by agent i. The inter-agent range has not been considered and plays no part in the measurement of α_i or the control law to be derived. The relevant parameters are shown in Figure 1.

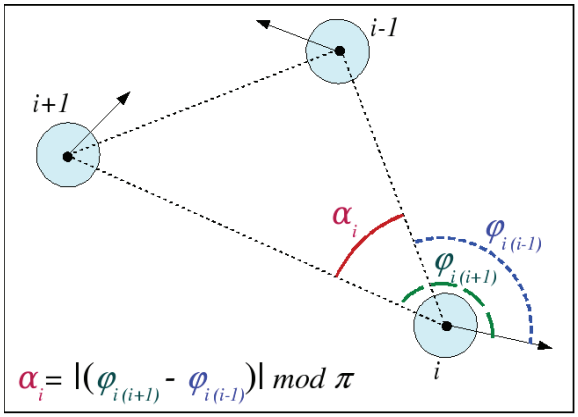

Fig. 1. Agent i computes α_i from the bearing measurements taken in a local coordinate system.

Define the desired steady-state angles $\alpha_i^* \in [0, \pi]$, $\forall i \in \mathcal{V}$. The α_i^* then completely characterize the shape (not scale) of the *desired* triangle formation.

Assumption 1. *The desired (i.e. control objective) interior angular separations α_i^*, obey $\alpha_1^* + \alpha_2^* + \alpha_3^* = \pi$.*

The assumption ensures the desired steady-state triangle is well-defined and the set of control objectives are simultaneously feasible.

A. The Proposed Control Law

The motion of agent i is governed by

$$\dot{\mathbf{p}}_i = v_i \begin{bmatrix} \cos\beta_i \\ \sin\beta_i \end{bmatrix} \tag{2}$$

where both v_i and β_i are control inputs to be determined. The heading β_i is measured positive (negative) counter-clockwise (clockwise) from agent i's local x_i-direction. The control law which determines v_i and β_i is truly distributed and determined solely by α_i^* and the measured angle α_i. The speed control input of agent i is defined as follows,

$$v_i = (\alpha_i^* - \alpha_i)k \tag{3}$$

where $k > 0$ is a constant (which in this paper is taken to be $k = 1$). The heading of agent i is defined along the bisection of $\alpha_i \in [0, \pi]$ and toward the interior of α_i so that

$$\beta_i = \begin{cases} \frac{\alpha_i}{2} + \min(\phi_{i(i+1)}, \phi_{i(i-1)}), & \text{if } \vartheta_i \le \pi \\ \frac{\alpha_i}{2} + \max(\phi_{i(i+1)}, \phi_{i(i-1)}), & \text{if } \vartheta_i > \pi \end{cases} \tag{4}$$

where

$$\vartheta_i = |\phi_{i(i+1)} - \phi_{i(i-1)}| \in [0, 2\pi) \tag{5}$$

is the angle subtended at agent i by agents $i+1$ and $i-1$ which is measured positive from the $\min(\phi_{i(i+1)}, \phi_{i(i-1)})$ to $\max(\phi_{i(i+1)}, \phi_{i(i-1)})$. Actually, it is easier to visualize the heading of agent i then to mathematically define it. Visually, the heading of agent i is simply toward the interior of α_i and specifically along the bisection of α_i. Of course, the speed of agent i might be negative. By definition, if $\alpha_i = \pi$ then the bisection is well defined by $\frac{\alpha_i}{2} + \min(\phi_{i(i+1)}, \phi_{i(i-1)})$. If $\alpha_i = 0$ then the bisection is also well defined.

B. Stability Analysis for the Proposed Control Law

The inter-agent range $r_{ij} = r_{ji} = \|\mathbf{p}_i - \mathbf{p}_j\|$ will be useful in analyzing the evolution of the multi-agent system but is not included in the implementation of the controller.

Consider agent i with $v_i = \alpha_i^* - \alpha_i$ and heading β_i defined as before (4) and note that $\mathcal{N}_i = \{(i+1), (i-1)\}$. Obviously, agent i moves with a speed of $\alpha_i^* - \alpha_i$ and with a heading along the bisection of α_i. Accordingly, $\dot{\alpha}_i$ is affected directly by $\alpha_i^* - \alpha_i$ and is given by

$$\dot{\alpha}_i = \frac{\sin(\alpha_{i+1}) + \sin(\alpha_{i-1})}{r_{i(i+1)}\sin(\alpha_{i+1})} \sin(\frac{\alpha_i}{2})(\alpha_i^* - \alpha_i) \tag{6}$$

when agents $i+1$ and $i-1$ are stationary. An equivalent expression for $\dot{\alpha}_i$, assuming $i+1$ and $i-1$ are static, is

$$\dot{\alpha}_i = \frac{\sin(\alpha_{i+1}) + \sin(\alpha_{i-1})}{r_{i(i-1)}\sin(\alpha_{i-1})} \sin(\frac{\alpha_i}{2})(\alpha_i^* - \alpha_i) \tag{7}$$

However, the movement of agents $i+1$ and $i-1$ also (directly) affects how $\dot{\alpha}_i$ evolves. To see this consider agent i moving with a speed of $\alpha_i^* - \alpha_i$ and with a heading along the bisection of α_i. If agents $i+1$ and $i-1$ are static, then

$$\dot{\alpha}_{i+1} = \frac{1}{r_{i(i+1)}} \sin(\frac{\alpha_i}{2})(\alpha_i^* - \alpha_i) \tag{8}$$

and similarly

$$\dot{\alpha}_{i-1} = \frac{1}{r_{i(i-1)}} \sin(\frac{\alpha_i}{2})(\alpha_i^* - \alpha_i) \tag{9}$$

Now for future notational brevity let

$$f_{i(i+1)} = \frac{1}{r_{i(i+1)}} \sin(\frac{\alpha_{i+1}}{2}) \tag{10}$$

and let

$$\begin{aligned} g_i &= \frac{\sin(\alpha_{i+1}) + \sin(\alpha_{i-1})}{r_{i(i+1)}\sin(\alpha_{i+1})} \sin(\frac{\alpha_i}{2}) \\ &= \frac{r_{i(i+1)} + r_{i(i-1)}}{r_{i(i+1)} r_{i(i-1)}} \sin(\frac{\alpha_i}{2}) \\ g_i &= \frac{\sin(\alpha_{i+1}) + \sin(\alpha_{i-1})}{r_{i(i-1)}\sin(\alpha_{i-1})} \sin(\frac{\alpha_i}{2}) \end{aligned} \tag{11}$$

where we note $g_i \ge 0$ and $f_{ij} \ge 0$ for all $i, j \in \{1, 2, 3\}$ when $\alpha_i \in [0, \pi]$, $\forall i$. Now, assuming all agents move with a motion governed by their individual control laws we have

$$\dot{\alpha}_i = g_i(\alpha_i^* - \alpha_i) - f_{i(i+1)}(\alpha_{i+1}^* - \alpha_{i+1}) - f_{i(i-1)}(\alpha_{i-1}^* - \alpha_{i-1}) \tag{12}$$

with $\alpha_i \in [0, \pi]$. Note that $\dot{\alpha}_i$ is well-defined for all $\alpha_i \in [0, \pi]$. The system of differential equations

$$\dot{\alpha} = \begin{bmatrix} -g_1 & f_{12} & f_{13} \\ f_{21} & -g_2 & f_{23} \\ f_{31} & f_{32} & -g_3 \end{bmatrix} \left(\alpha - \begin{bmatrix} \alpha_1^* \\ \alpha_2^* \\ \alpha_3^* \end{bmatrix} \right) \tag{13}$$

where

$$\alpha = \begin{bmatrix} \alpha_1 & \alpha_2 & \alpha_3 \end{bmatrix}^{\mathrm{T}} \tag{14}$$

is defined on a 2-simplex (without part of the boundary) in α-space with vertices $\alpha = [\pi\ 0\ 0]^\top$, $\alpha = [0\ \pi\ 0]^\top$ and $\alpha = [0\ 0\ \pi]^\top$. We denote this manifold by $\mathcal{M}_\alpha$.

Define the control error $e_i = (\alpha_i - \alpha_i^*) \in [-\pi, \pi]$ for each agent i. Then the following differential system is obtained

$$\begin{aligned} \dot{e}_i &= -\frac{\sin(\alpha_{i+1}) + \sin(\alpha_{i-1})}{r_{i(i+1)}\sin(\alpha_{i+1})}\sin(\frac{\alpha_i}{2})e_i + \\ &\quad \frac{e_{i+1}}{r_{i(i+1)}}\sin(\frac{\alpha_{i+1}}{2}) + \frac{e_{i-1}}{r_{i(i-1)}}\sin(\frac{\alpha_{i-1}}{2}) \end{aligned} \tag{15}$$

Using both (10) and (11), then the system of differential equations (15) can be written succinctly as

$$\dot{e}_i = -g_i e_i + f_{i(i+1)}e_{i+1} + f_{i(i-1)}e_{i-1} \tag{16}$$

Note that $\dot{e}_i$ is a nonlinear differential equation since $\alpha_i = \alpha_i^* + e_i$. Stacking the system (15) or (16) leads to

$$\dot{\mathbf{e}} = \mathbf{F}(\mathbf{e})\mathbf{e} \tag{17}$$

where $\mathbf{e} = \begin{bmatrix} e_1 & e_2 & e_3 \end{bmatrix}^{\mathrm{T}}$ and where

$$\mathbf{F}(\mathbf{e}) = \begin{bmatrix} -g_1 & f_{12} & f_{13} \\ f_{21} & -g_2 & f_{23} \\ f_{31} & f_{32} & -g_3 \end{bmatrix} \tag{18}$$

where $\mathbf{e}$ is defined on a 2-simplex in $\mathbf{e}$-space with vertices $\mathbf{e} = [\pi - \alpha_1^*\ -\alpha_2^*\ -\alpha_3^*]^\top$, $\mathbf{e} = [-\alpha_1^*\ \pi - \alpha_2^*\ -\alpha_3^*]^\top$ and $\mathbf{e} = [-\alpha_1^*\ -\alpha_2^*\ \pi - \alpha_3^*]^\top$. We denote this manifold by $\mathcal{M}_e$.

Figure 2 depicts the error manifold and shows six distinct error regions, $\mathfrak{R}_{i\pm}$, with $i \in \{1, 2, 3\}$.

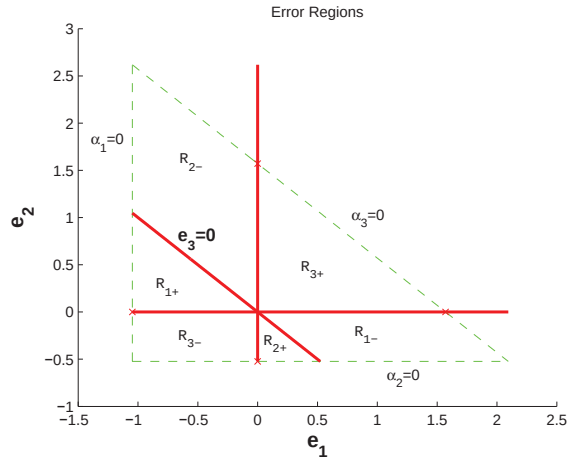

Fig. 2. The error manifold showing six distinct regions and the boundaries.

Note the regions are taken without boundary such that, for example, we can define $\mathfrak{R}_{3+}$ by

$$\mathbf{e} \in \mathfrak{R}_{3+} \iff \begin{bmatrix} 0 < e_1 < \pi - \alpha_1^* \\ 0 < e_2 < \pi - \alpha_2^* \\ -\alpha_3^* < e_3 < 0 \end{bmatrix} \tag{19}$$

For distinct $i, j, k \in \{1, 2, 3\}$, we chose the individual error regions to exhibit the following useful properties

$$\mathfrak{R}_{i+} \Rightarrow \{e_j > 0, e_k > 0, e_i < 0, \dot{e}_i > 0\} \tag{20}$$

$$\mathfrak{R}_{i-} \Rightarrow \{e_j < 0, e_k < 0, e_i > 0, \dot{e}_i < 0\} \tag{21}$$

where $e_i \in [-\alpha_i^*, \pi - \alpha_i^*] \subset [-\pi, \pi]$, $\forall i$ and $\sum_i e_i = 0$ must be enforced. The sign of the errors is taken directly from the definition of the region while the sign of a particular error velocity can be determined using the signs of the error and (17). *The inequalities are strict*. Note importantly that the simplex, or manifold $\mathcal{M}_e$ shifts in the error space depending on the desired configuration angles α_i^*. As such, error regions, $\mathfrak{R}_{i\pm}$, can grow or shrink, and can disappear altogether. For example, take the case where $\alpha_1^* = \alpha_2^* = 0$ such that $\alpha_3^* = \pi$, then the only region in existence is $\mathfrak{R}_{3+}$.

Theorem 1. *The manifold $\mathcal{M}_e$ is a positively invariant set for the system (17).*

Proof: To show that $\mathcal{M}_e$ is positively invariant we show that for any $e_i \in \mathcal{M}_e$, then it is impossible for e_i to escape $\mathcal{M}_e$. Note that $e_i \in [-\alpha_i^*, \pi - \alpha_i^*] \subset [-\pi, \pi]$. Thus, let us consider the right-sided limit,

$$\begin{aligned} \lim_{e_i \to -\alpha_i^{*+}} \dot{e}_i &= \frac{1}{r_{i(i+1)}}\sin(\frac{\alpha_{(i+1)}}{2})e_{i+1} + \\ &\quad \frac{1}{r_{i(i-1)}}\sin(\frac{\alpha_{(i-1)}}{2})e_{i-1} \\ &= \frac{e_{i+1}}{r_{i(i+1)}} \quad \text{if} \quad \begin{matrix} e_{i+1} \to (\pi - \alpha_{i+1}^*)^- \\ e_{i-1} \to -\alpha_{i-1}^{*+} \end{matrix} \\ &= \frac{e_{i-1}}{r_{i(i-1)}} \quad \text{if} \quad \begin{matrix} e_{i+1} \to -\alpha_{i+1}^{*+} \\ e_{i-1} \to (\pi - \alpha_{i-1}^*)^- \end{matrix} \\ &> 0 \end{aligned} \tag{22}$$

which implies e_i cannot escape $\mathcal{M}_e$ in one direction. A similar computation shows that e_i cannot escape $\mathcal{M}_e$ in the other direction, i.e. by following $e_i \to \pi - \alpha_i^*$ through the boundary of the manifold. That is

$$\begin{aligned} \lim_{e_i \to (\pi - \alpha_i^*)^-} \dot{e}_i &= -\frac{r_{i(i+1)} + r_{i(i-1)}}{r_{i(i+1)}r_{i(i-1)}}e_i \\ &< 0 \end{aligned} \tag{23}$$

which completes the proof. ∎

We state the following result which ensures the formation is well-defined for all time t, i.e. the angles α_i are well defined for all time. The next result proves collisions are impossible.

Theorem 2. *Suppose that $\mathbf{p}_i(t_0) \neq \mathbf{p}_j(t_0)$ for $i \neq j$ at some time t_0. Then, $\mathbf{p}_i(t) \neq \mathbf{p}_j(t)$ for $i \neq j$ for all $t \geq t_0$, i.e. for all $t \geq t_0$ we have $\|\mathbf{p}_i(t) - \mathbf{p}_j(t)\| > 0$.*

Proof: In order for $\mathbf{p}_i(t) = \mathbf{p}_j(t)$ at some time $t > t_0$ there must exist a time interval $[t - \epsilon, t]$ with $t - \epsilon \geq t_0$ on which $\beta_i = \phi_{ij}$ and/or $\beta_j = \phi_{ji}$ for any $\epsilon \geq dt$. We now show that no such time interval can exist. We consider now, with no loss of generality, that $\beta_i = \phi_{ij}$. Note that $\beta_i = \phi_{ij}$ on $[t-\epsilon, t]$ then implies $\alpha_i = 0$ which implies $\alpha_j = 0$ or $\alpha_j = \pi$ on the entire interval $[t-\epsilon, t]$. If $\alpha_j(t-\epsilon) = \pi$ then at time $t-\epsilon+dt$

we immediately have $\beta_i \neq \phi_{ij}$ since $\alpha_j(t-\epsilon+dt) < \pi$. To see this note that $\alpha_j(t-\epsilon) = \pi$ implies

$$\dot{\alpha}_j = -g_j(\alpha_j - \alpha_j^*) \;\text{ on }\; [t-\epsilon, t-\epsilon+dt] \tag{24}$$

which is strictly negative unless $\alpha_j^* = \pi$ which according to Assumption 1 would imply that both agents $i, k \neq j$ are also at equilibrium. Similarly, if $\alpha_j = 0$ then at time $t-\epsilon+dt$ we immediately have $\beta_i \neq \phi_{ij}$ since $\alpha_j(t-\epsilon+dt) > 0$. ■

The following result characterizes the equilibrium points of the system.

Theorem 3. *The system (17) is at equilibrium $\dot{\mathbf{e}} = 0$ on $\mathcal{M}_e$ if and only if $\mathbf{e} = 0$.*

Proof: The sufficiency of $\mathbf{e} = 0$ is obvious. Now assume that $e_i \neq 0$ for all $i \in \{1,2,3\}$ and suppose $\dot{\mathbf{e}} = 0$. We now proceed via a contradiction. The state of the system is in one of the six distinct regions $\mathfrak{R}_{\mathrm{i}+}$ or $\mathfrak{R}_{\mathrm{i}-}$ defined using (20) or (21). Using (20) or (21) it is clear $\dot{e}_i \neq 0$ for at least one i, i.e. contradicting our assumption $\dot{\mathbf{e}} = 0$.

Now it remains to show that on the manifold $\mathcal{M}_e$ there are no equilibrium points on the boundaries in between the error regions. Denote such a boundary via

$$\Sigma_{\mathrm{i+j-}} = \{\partial\mathfrak{R}_{\mathrm{i}+} \cap \partial\mathfrak{R}_{\mathrm{j}-}\}/\{\mathbf{0}\} = \Sigma_{\mathrm{j-i+}} \tag{25}$$

and note we consider only boundaries with strictly positive length, i.e. a strictly positive 1-d Hausdorff measure. Now following our derivation of the error regions $\mathfrak{R}_{\mathrm{i}+}$ we find that

$$\mathbf{e} \in \Sigma_{\mathrm{i+j-}} \iff \begin{bmatrix} -\alpha_i^* < e_i < 0 \\ 0 < e_j < \pi - \alpha_j^* \\ e_k = 0 \end{bmatrix} \tag{26}$$

which implies, using (16), that $\dot{e}_i > 0$ and $\dot{e}_j < 0$ and thus $\dot{\mathbf{e}} \neq 0$. This completes the proof. ■

We now introduce the following theorem which will form the basis of our subsequent stability proof.

Theorem 4 (Poincare-Bendixson [19])**.** *Let $\mathcal{M} \subset \mathbb{R}^2$ be a compact, positively invariant two-manifold containing a finite number of fixed points. Let $\mathbf{x} \in \mathcal{M}$ and consider the ω-limit set $\omega(\mathbf{x})$. Then one of the following possibilities holds:*

1) *$\omega(\mathbf{x})$ is an equilibrium point;*
2) *$\omega(\mathbf{x})$ is a closed orbit;*
3) *$\omega(\mathbf{x})$ consists of a finite number of fixed points $\overline{\mathbf{x}}_1, \ldots, \overline{\mathbf{x}}_m$ and orbits γ with $\alpha(\gamma) = \overline{\mathbf{x}}_i$ and $\omega(\gamma) = \overline{\mathbf{x}}_j$,*

where $\alpha(\gamma)$ means the α-limit set of every point γ.

The intuition behind the Poincare-Bendixson theorem is that all bounded trajectories in a planar region (or two-manifold) must converge to an equilibrium point, a limit cycle, or a union of fixed points and the trajectories connecting them, i.e. so-called homoclinic or heteroclinic orbits.

We know there is only a single equilibrium and that $\mathcal{M}_e$ is positively invariant. We now show there are no closed orbits.

Theorem 5. *The system (17) has no closed orbits in $\mathcal{M}_e$.*

Proof: Consider the arc between adjacent regions given by

$$\Sigma_{\mathrm{i+j-}} = \{\partial\mathfrak{R}_{\mathrm{i}+} \cap \partial\mathfrak{R}_{\mathrm{j}-}\}/\{\mathbf{0}\} = \Sigma_{\mathrm{j-i+}} \tag{27}$$

with strictly positive length, i.e. a strictly positive 1-d Hausdorff measure. There are six such 'well-defined' sets $\Sigma_{\mathrm{i+j-}} = \Sigma_{\mathrm{j-i+}}$. Now define

$$\begin{aligned}\Sigma = \Sigma_{3+1-} \cup \Sigma_{1-2+} \cup \Sigma_{2+3-} \cup \\ \Sigma_{3-1+} \cup \Sigma_{1+2-} \cup \Sigma_{2-3+}\end{aligned} \tag{28}$$

and note for clarity that $\Sigma \cap \{\mathbf{0}\} = \emptyset$. Note that any closed orbit must enclose the origin [19] and thus intersect every well-defined boundary $\Sigma_{\mathrm{i+j-}}$. The strategy is to show that any positive orbit $\psi^+(\mathbf{e})$ of (17) intersects Σ in a strictly monotone sequence approaching the origin (if it intersects it in more than point). That is, we show that if $\mathbf{e}_{m+1}$ is the $(m+1)^{\text{th}}$ intersection of Σ then $\|\mathbf{e}_{m+1}\| < \|\mathbf{e}_m\|$. Note that

$$\begin{aligned}\mathbf{e} \in \Sigma_{\mathrm{i+j-}} \;&\Rightarrow\; \dot{e}_i > 0,\ e_i < 0 \;\text{ and }\; \dot{e}_j < 0,\ e_j > 0 \\ &\Rightarrow\; e_k = 0 \;\text{ and }\; \|\mathbf{e}\| = |e_j|\end{aligned} \tag{29}$$

using the definition of regions where $i, j, k \in \{1,2,3\}$ are distinct indices. We proceed using an inductive-like argument. Suppose that $\mathbf{e}_m$ is the m^{th} intersection of Σ (which also intersects $\Sigma_{\mathrm{i+j-}}$) for the positive orbit $\psi_t^+(\mathbf{e}_m)$ starting at $t = t_m$. Define a time t_{m+1} and mark $\mathbf{e}_{m+1}$ as the $(m+1)^{\text{th}}$ intersection of Σ with $\mathbf{e}_{m+1} = \psi^+_{t_{m+1}}(\mathbf{e}_m)$. There exists a time $t_{m^+} \in (t_m, t_{m+1}]$ at which $\psi^+_{t_{m^+}}(\mathbf{e}_m)$ is in (i) $\Sigma_{\mathrm{i+j-}}$ or (ii) $\mathfrak{R}_{i+}$ or (iii) $\mathfrak{R}_{j-}$. We ignore the trivial case $\psi^+_{t_{m^+}}(\mathbf{e}_m) \in \{\mathbf{0}\}$ for some $t_{m^+} \in (t_m, t_{m+1})$.

(Case i): If $\psi^+_{t_{m^+}}(\mathbf{e}_m)$ is in $\Sigma_{\mathrm{i+j-}}$ then $t_{m^+} = t_{m+1}$ and $0 < e_j(t_{m+1}) < e_j(t_m)$ using (29). It follows that $\|\mathbf{e}_{m+1}\| < \|\mathbf{e}_m\|$. We restart the argument at time $t = t_{m+1}$.

(Case ii): If $\psi^+_{t_{m^+}}(\mathbf{e}_m)$ is in $\mathfrak{R}_{i+}$ then $e_j > 0$, $e_k > 0$ and $\dot{e}_i = -\dot{e}_j - \dot{e}_k > 0$ which implies $-\dot{e}_j > \dot{e}_k$. The relevant boundaries of $\mathfrak{R}_{i+}$ are $\Sigma_{\mathrm{i+j-}}$ and $\Sigma_{\mathrm{i+k-}}$ for distinct $i, j, k \in \{1,2,3\}$. Now if $\mathbf{e}_{m+1} \in \Sigma_{\mathrm{i+j-}}$ then

$$\int_{t_m}^{t_{m+1}} \dot{e}_k(\tau)d\tau = 0 \;\Rightarrow\; \int_{t_m}^{t_{m+1}} \dot{e}_j(\tau)d\tau < 0 \tag{30}$$

which immediately implies $|e_j(t_{m+1})| < |e_j(t_m)|$. Using (29) it follows that $\|\mathbf{e}_{m+1}\| < \|\mathbf{e}_m\|$ and we can then restart the argument at time $t = t_{m+1}$. Now if instead $\mathbf{e}_{m+1} \in \Sigma_{\mathrm{i+k-}}$ then $-\dot{e}_j > \dot{e}_k$ implies

$$\int_{t_m}^{t_{m+1}} \dot{e}_j(\tau)d\tau = -e_j(t_m) \;\Rightarrow\; \int_{t_m}^{t_{m+1}} \dot{e}_k(\tau)d\tau < e_j(t_m) \tag{31}$$

and since $e_k(t_m) = 0$ we have $|e_k(t_{m+1})| < |e_j(t_m)|$. The consequence of this last fact is that $\|\mathbf{e}_{m+1}\| < \|\mathbf{e}_m\|$ and we can then restart the argument at time $t = t_{m+1}$.

(Case iii): If $\psi^+_{t_{m^+}}(\mathbf{e}_m)$ is in $\mathfrak{R}_{j-}$ then the argument follows similarly to that given in case (ii). The proof is complete. ■

Note that Theorem 5 could be interpreted as a proof of asymptotic convergence of any solution of (17) to the origin. The following result makes this convergence precise.

Theorem 6. *The equilibrium* $\mathbf{e} = 0$ *of the error system (17) is globally asymptotically stable.*

Proof: We use the Poincare-Bendixson theorem. Consider $\mathcal{M}_e^- = \mathrm{cl}(\mathcal{M}_e)$ where $\mathrm{cl}(\cdot)$ denotes the set closure operation. Note that $\mathcal{M}_e^-$ is now compact with a single equilibrium and no closed orbits. Note $\mathcal{M}_e$ is not closed (or completely open). However, $\mathbf{e}(0)$ must be in $\mathcal{M}_e \subset \mathcal{M}_e^-$ and we say $\mathcal{M}_e^-$ acts as a positively invariant set. The Poincare-Bendixson theorem states that the ω-set of any initial condition in $\mathcal{M}_e^-$ contains only $\mathbf{e} = 0$. Thus, global asymptotic stability is assured. ■

C. Discussion on the Method of Proof

Note we could not find a suitable Lyapunov function that would prove global stability for all desired formations given any initial configuration. In particular, testing the negative-definiteness of the time-derivative for various candidates was a significant hurdle. Variations on a number of quadratic-type candidate functions failed the negative-definite test in simulation. However, it was clear to us that the system evolved on a positively-invariant set and that there was only a single equilibrium. Moreover, we suspected that no limit cycles were present. As such, given the dimension of the system manifold, we know the Poincare-Bendixson theorem provides a rigorous statement concerning the asymptotic behavior of the system trajectories. Thus, we chose to seek an asymptotic convergence proof through the Poincare-Bendixson theorem which subsequently provides a deep insight into the nature of the dynamical system.

D. Robustness to a Single Agent Motion Failure

The proposed distributed control law is generally robust to a single agent motion failure, i.e. the failure of a single agent to move in the presence of a non-zero control error. With no loss of generality, assume agent 1 cannot move in space. However, assume that α_i^* is still specified for all $i \in \mathcal{V}$ and that, in general, $\alpha_i(0) \neq \alpha_i^*$, for all i. Agents 2 and 3 both implement the previously designed control law and each considers only its own control error $\alpha_i - \alpha_i^*$ in the construction of its control signal. The modified error system takes the form

$$\dot{\mathbf{e}} = \begin{bmatrix} 0 & f_{12} & f_{13} \\ 0 & -g_2 & f_{23} \\ 0 & f_{32} & -g_3 \end{bmatrix} \mathbf{e} \tag{32}$$

where $\mathbf{e} = \begin{bmatrix} e_1 & e_2 & e_3 \end{bmatrix}^{\mathrm{T}}$ and where $\dot{\mathbf{e}}$ evolves on $\mathcal{M}_e$.

Theorem 7. *Assume agent* 1 *suffers a motion failure and does not move in space, i.e. neglects any control law design. Assume that* $\alpha_1(0) \neq \pi$ *and* $\alpha_i(0) \neq 0$ *for* $i \in \{2, 3\}$. *The equilibrium* $\mathbf{e} = 0$ *of the system (32) is globally asymptotically stable.*

Proof: The proof is omitted for brevity. ■

Note that initial line formations cannot be allowed if the agent experiencing motion failure is in between the remaining two agents (because the remaining two agents will drive directly toward the agent experiencing motion failure until collision, i.e. until at least two agents become collocated).

III. Examples

We demonstrate the algorithm for distributed formation control with bearing-only measurements and angular constraints.

1) Triangle to Triangle Formation: The first example shows how the formation converges to an arbitrarily desired (feasible) triangle given a random initial triangle configuration. The desired formation is characterized by $\alpha_1^* = \pi/6$, $\alpha_2^* = \pi/4$ and $\alpha_3^* = 7\pi/12$. The formation motion is illustrated in Figure 3 along with the convergence of $|e_i|$ to zero.

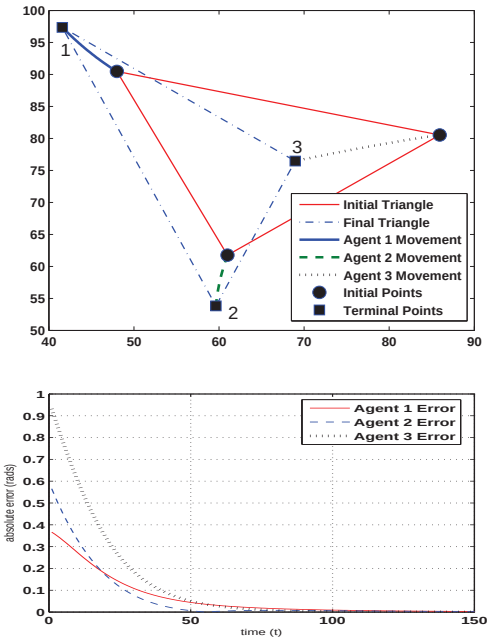

Fig. 3. The motion of the formation with a desired terminal constraint of $\alpha_1^* = \pi/6$, $\alpha_2^* = \pi/4$ and $\alpha_3^* = 7\pi/12$.

The initial position of the three agents are randomly distributed in $\mathcal{M}_\alpha$ and the figure illustrates the trajectories of each agent as the formation converges upon the desired shape.

2) Line to Triangle Formation: Consider now the case involving three agents initially collinear. The desired formation is a triangle characterized by $\alpha_1^* = \pi/3$, $\alpha_2^* = \pi/6$ and $\alpha_3^* = \pi/2$. The formation motion is illustrated in Figure 4 along with the control error for each agent.

The convergence of the three agents is illustrated in Figure 4 along with the convergence of $|e_i|$ to zero for all $i \in \{1, 2, 3\}$. This example illustrates that the control law is not affected by initial agent collinearity.

3) Triangle to Line Formation: The final example shows the convergence of an initially random triangle formation to a desired line formation. The desired formation is characterized by $\alpha_1^* = \alpha_2^* = 0$ and $\alpha_3^* = \pi$.

The convergence of the three agents is illustrated in Figure 5 along with the convergence of $|e_i|$ to zero for all $i \in \{1, 2, 3\}$. This example illustrates that we can steer an arbitrary initial triangle formation to a collinear formation.

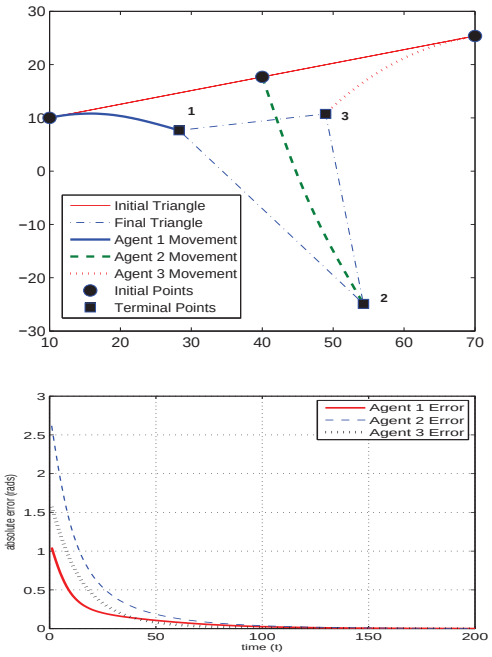

Fig. 4. The motion of a triangular formation consisting of three mobile agents initially in a collinear position with desired terminal constraints $\alpha_1^* = \pi/3$, $\alpha_2^* = \pi/6$ and $\alpha_3^* = \pi/2$.

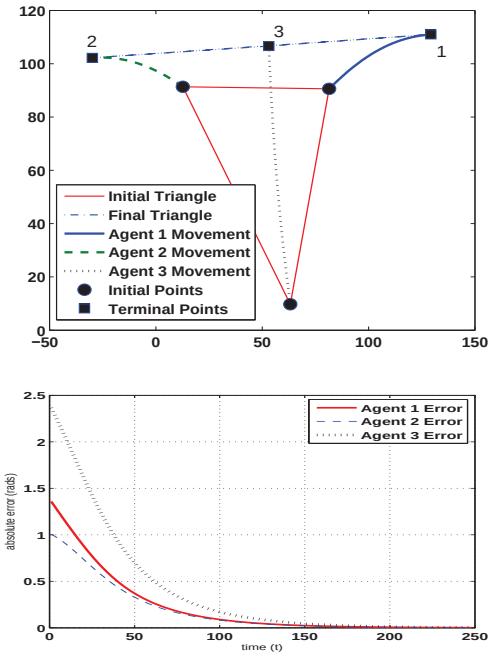

Fig. 5. The motion of a triangular formation consisting of three mobile agents starting in a random triangle and given a desired collinearity condition.

IV. Conclusion

This paper introduced a solution to the distributed bearing-only triangular formation control problem with angle-only inter-agent constraints. While the distance-based formation control problem has been extensively considered in the literature, the problem of bearing-only formation control is less studied. The solution provided in this paper requires only that each agent measure the bearing to the remaining two agents in a local coordinate system. Given a set of desired interior angles, then the group of agents is shown to converge to the desired formation from any initial position.

References

[1] A.N. Bishop, B. Fidan, B.D.O. Anderson, K. Dogancay, and P.N. Pathirana. Optimality analysis of sensor-target geometries in passive localization: Part 1 - Bearing-only localization. In *Proc. of the 3rd International Conference on Intelligent Sensors, Sensor Networks, and Information Processing*, Melbourne, Australia, December 2007.

[2] A.N. Bishop, B. Fidan, B.D.O. Anderson, P.N. Pathirana, and K. Dogancay. Optimality analysis of sensor-target geometries in passive localization: Part 2 - Time-of-arrival based localization. In *Proc. of the 3rd International Conference on Intelligent Sensors, Sensor Networks, and Information Processing*, Melbourne, Australia, December 2007.

[3] A. Jadbabaie, J. Lin, and A.S. Morse. Coordination of groups of mobile autonomous agents using nearest neighbor rules. *IEEE Transactions on Automatic Control*, 48(6):988–1001, June 2003.

[4] A.V. Savkin. Coordinated collective motion of groups of autonomous mobile robots: Analysis of Vicsek's model. *IEEE Transactions on Automatic Control*, 49(6):981–983, June 2004.

[5] J.A. Fax and R.M. Murray. Information flow and cooperative control of vehicle formations. *IEEE Transactions on Automatic Control*, 49(9):1464–1476, September 2004.

[6] J. Cortes, S. Martinez, and F. Bullo. Robust rendezvous for mobile agents via proximity graphs in arbitrary dimensions. *IEEE Transactions on Automatic Control*, 51(8):1289–1298, August 2006.

[7] R. Olfati-Saber. Flocking for multi-agent dynamic systems: Algorithms and theory. *IEEE Transactions on Automatic Control*, 51(3):401–420, March 2006.

[8] V. Gazi. Stability analysis of swarms. *IEEE Transactions on Automatic Control*, 48(4):692–697, April 2003.

[9] E. Rimon and D.E. Koditschek. Exact robot navigation using artificial potential functions. *IEEE Transactions on Robotics and Automation*, 8(5):501–518, October 1992.

[10] Z. Lin, M.E. Broucke, and B.A. Francis. Local control strategies for groups of mobile autonomous agents. *IEEE Transactions on Automatic Control*, 49(4):622–629, April 2004.

[11] R. O. Saber and R. M. Murray. Graph rigidity and distributed formation stabilization of multi-vehicle systems. In *Proceedings of the 41st IEEE Conference on Decision and Control*, pages 2965–2971, Las Vegas, Nevade, USA, 2002.

[12] J. Baillieul and A. Suri. Information patterns and hedging Brockett's theorem controlling vehicle formations. In *Proceedings of the 42nd IEEE Conference on Decision and Control*, pages 556–563, Maui, Hawaii, USA, December 2003.

[13] Z. Lin, B.A. Francis, and M. Maggiore. Necessary and sufficient graphical conditions for formation control of unicycles. *IEEE Transactions on Automatic Control*, 50(1):121–127, January 2005.

[14] B.D.O Anderson, C. Yu, S. Dasgupta, and A.S. Morse. Control of a three-coleader formation in the plane. *Systems and Control Letters*, 56(9-10):573–578, 2007.

[15] S.C. Nardone, A.G. Lindgren, and K.F. Gong. Fundamental properties and performance of conventional bearings-only target motion analysis. *IEEE Transactions on Automatic Control*, 29(9):775–787, 1984.

[16] M. Gavish and A.J. Weiss. Performance analysis of bearing-only target location algorithms. *IEEE Transactions on Aerospace and Electronic Systems*, 28(3):817–827, 1992.

[17] A.N. Bishop, B. Fidan, K. Dogancay, B.D.O. Anderson, and P.N. Pathirana. Exploiting geometry for improved hybrid AOA/TDOA based localization. *Signal Processing*, 88(7):1775–1791, July 2008.

[18] A.N. Bishop, B. Fidan, B.D.O. Anderson, P.N. Pathirana, and G. Mao. Bearing-only localization using geometrically constrained localization. *IEEE Transactions on Aerospace and Electronic Systems*, 45(1):308–320, January 2009.

[19] S. Wiggins. *Introduction to Applied Nonlinear Dynamical Systems and Chaos*. Springer-Verlag, New York, NY, 1990.